Journal of Nuclear Medicine, published on February 14, 2011 as doi:10.2967/jnumed.110.077479

Monitoring Tumor Response to Antiangiogenic Sunitinib Therapy with ^{18}F-Fluciclatide, an ^{18}F-Labeled $\alpha_V\beta_3$-Integrin and $\alpha_V\beta_5$-Integrin Imaging Agent

Mark R. Battle*, Julian L. Goggi*, Lucy Allen, Jon Barnett, and Matthew S. Morrison

GE Healthcare MDx Research, The Grove Centre, Amersham, United Kingdom

Arginine-glycine-aspartate (RGD)-binding $\alpha_V\beta_3$-integrin and $\alpha_V\beta_5$-integrin play key roles in tumor angiogenesis. We examined an ^{18}F-labeled small peptide (fluciclatide [United States Adopted Name (ASAN)–approved, International Nonproprietary Name (INN)–proposed name], previously referred to as AH111585) containing an RGD sequence. Fluciclatide binds with a high (nM) affinity to $\alpha_V\beta_3$-integrin and $\alpha_V\beta_5$-integrin, which are highly expressed on tumors and the tumor neovasculature. In this study, ^{18}F-fluciclatide was used to examine the response of human glioblastoma xenografts to treatment with the antiangiogenic agent sunitinib. **Methods:** U87-MG tumor uptake of ^{18}F-fluciclatide was determined by small-animal PET after longitudinal administration of the antiangiogenic agent sunitinib (a 2-wk dosing regimen). Tumor sizes were measured throughout the study, and tumor volumes were calculated. Tumor microvessel density (MVD) after therapy was also analyzed. **Results:** Dynamic small-animal PET of ^{18}F-fluciclatide uptake after administration of the clinically relevant antiangiogenic agent sunitinib revealed a reduction in the tumor uptake of ^{18}F-fluciclatide compared with that in vehicle-treated controls over the 2-wk dosing regimen. Skeletal muscle, used as a reference tissue, showed equivalent ^{18}F-fluciclatide uptake in both therapy and control groups. A reduction in tumor MVD was also observed after treatment with the antiangiogenic agent. No significant changes in tumor volume were observed in the 2 groups. **Conclusion:** The data demonstrated that ^{18}F-fluciclatide detected changes in tumor uptake after acute antiangiogenic therapy markedly earlier than any significant volumetric changes were observable. These results suggest that this imaging agent may provide clinically important information for guiding patient care and monitoring the response to antiangiogenic therapy.

Key Words: ^{18}F-fluciclatide; sunitinib; PET; $\alpha_V\beta_3$-integrin; RGD peptide

J Nucl Med 2011; 52:424–430
DOI: 10.2967/jnumed.110.077479

Integrins are a family of cell adhesion molecules consisting of 2 noncovalently bound transmembrane subunits, α and β, that form heterodimers with distinct adhesive capabilities (*1*). In mammals, 18 α and 8 β subunits assemble into 24 different receptors. Integrins play important roles in several pathologic processes, such as inflammation, fibrosis, tumor metastasis, and angiogenesis (*2,3*).

Angiogenesis, the process of forming new blood vessels from existing vessels (*4*), is central to normal biologic processes, such as embryogenesis, tissue remodeling, inflammation, and wound healing, and is present in numerous disease states, including rheumatoid arthritis, psoriasis, restenosis, diabetic retinopathy, and tumor growth (*5–7*). The interest in angiogenesis research has been fueled by the potential to develop antiangiogenic drugs as novel therapeutic agents for targeting tumors and several nononcologic diseases.

$\alpha_V\beta_3$-integrin and $\alpha_V\beta_5$-integrin act as receptors for a variety of proteins expressing the exposed arginine-glycine-aspartate (RGD) tripeptide sequence, such as vitronectin, fibronectin, fibrinogen, laminin, collagen, Von Willebrand factor, osteoponin, and adenovirus particles (*2,8–11*). $\alpha_V\beta_3$-integrin and $\alpha_V\beta_5$-integrin are expressed at low levels on epithelial cells and mature endothelial cells but are expressed at high levels on activated endothelial cells in the neovasculature of a range of tumors, including osteosarcomas, neuroblastomas, glioblastomas, melanomas, lung carcinomas, and breast cancer (*2,12*). Additionally, the expression of $\alpha_V\beta_3$-integrin and $\alpha_V\beta_5$-integrin correlates well with tumor progression and the invasiveness of several tumors, such as melanomas, gliomas, neuroblastomas, and ovarian and breast cancers (*13–15*).

Others have shown that RGD peptides can serve as targeting biomolecules for carrying a range of radionuclides (e.g., ^{18}F, ^{99m}Tc, and ^{64}Cu) to RGD-binding integrins (such as $\alpha_V\beta_3$-integrin) that are upregulated in cancer (*16–21*). The PET tracer ^{18}F-fluciclatide is an ^{18}F-radiolabeled small peptide containing the RGD sequence. ^{18}F-fluciclatide is currently being developed as a radiotracer for the imaging of angiogenesis in tumors. ^{18}F-fluciclatide binds with a high affinity to RGD-binding $\alpha_V\beta_3$-integrin and $\alpha_V\beta_5$-integrin (*22*), which are upregulated during angiogenesis. Therefore,

Received Mar. 24, 2010; revision accepted Jul. 8, 2010.
For correspondence or reprints contact: Mark R. Battle, Discovery Biology, GE Healthcare Ltd., The Grove Centre, White Lion Rd., Amersham, Buckinghamshire HP7 9LL, U.K.
E-mail: mark.battle@ge.com
*Contributed equally to this work.

the uptake of ^{18}F-fluciclatide can be used to monitor the response of tumors to antiangiogenic drugs, such as sunitinib (Sutent; Pfizer Inc.).

At present, contrast-enhanced MRI and CT are commonly used to assess changes in tumor blood flow, permeability, and volume as a response to antiangiogenic therapies. However, these modalities provide a limited understanding of the full effects of targeting the tumor vasculature. The development of noninvasive imaging methods with radiolabeled tracers, such as ^{18}F-fluciclatide, would provide a means of determining quantitative changes in the tumor vasculature in patients with cancer.

The tracer ^{18}F-fluciclatide has the advantage of specific targeting of $\alpha_V\beta_3$-integrin and $\alpha_V\beta_5$-integrin in tumor angiogenesis. Other tracers, including ^{124}I-VG76e, ^{64}Cu-DOTA-VEGF$_{121}$, and ^{64}Cu-single-chain (sc)VEGF (as markers for vascular endothelial growth factor [VEGF] or VEGF receptors [VEGFRs] in tumor angiogenesis) as well as ^{18}F-NC100717, ^{11}C-NC100717, and ^{18}F-galacto-RGD (as $\alpha_V\beta_3$-integrin and $\alpha_V\beta_5$-integrin markers), have been developed and evaluated, but their advancement clinically has been limited (*23,24*). VEGF-targeted tracers have been used to determine the effects of therapies that inhibit or disrupt the vasculature within a tumor. The development of ^{18}F-fluciclatide may provide a means to examine the effects of vasculature-modulating therapies directly, without the reliance on consequential changes in blood perfusion and permeability within a tumor, especially with the progression of alternative (non-VEGF) therapies clinically.

The purpose of the present study was to longitudinally assess the effects of repeated administration of sunitinib, an antiangiogenic receptor tyrosine kinase inhibitor (*25–27*), on the uptake of ^{18}F-fluciclatide in glioblastoma xenograft tumor–bearing mice.

MATERIALS AND METHODS

Radiochemistry

The chemical synthesis of the precursor for ^{18}F-fluciclatide was described previously (*28*). Radiosynthesis was performed at GE Healthcare. A full description of the synthesis was published elsewhere (*29*). In brief, ^{18}F-fluoride was azeotropically dried in the presence of Kryptofix (K_{222}; Merck) (11 mg in 1.0 mL of acetonitrile) and potassium carbonate (1.4 mg in 1 mL of acetonitrile) by heating under a flow of nitrogen and placement in a vacuum for 15 min. Care was taken to ensure that all traces of acetonitrile were removed. The K_{222}–K^+–F^- complex was cooled to less than 40°C, and 4-trimethylammoniumbenzaldehyde (3 mg in 1 mL of dimethyl sulfoxide) was added. The reaction vessel was sealed and heated to 90°C for 15 min to effect radiolabeling. The crude *p*-^{18}F-fluorobenzaldehyde solution was cooled to room temperature, diluted with water, and passed through a solid-phase extraction cartridge; *p*-^{18}F-fluorobenzaldehyde was retained, and excess precursor, K_{222}, dimethyl sulfoxide, and hydrophilic by-products were eluted to waste. *p*-^{18}F-fluorobenzaldehyde was subsequently recovered in ethanol for conjugation with peptide.

The peptide precursor (5 mg of free-base–equivalent AH111695 [GE Healthcare], the RGD peptide with amino-oxy functionality (*29*)) was dissolved in 0.1 M phosphate/citrate solution (pH 2.5; 1.0 mL), and this solution was combined with the purified *p*-^{18}F-fluorobenzaldehyde solution in a reaction vessel. The vessel was sealed and heated to 70°C for 15 min to effect conjugation. After the crude conjugate was cooled to room temperature, it was purified by preparative high-performance liquid chromatography (Viva C4 [Restek]; 5 μm, 100 × 4.6 mm; 0.1% H_3PO_4:ethanol 75:25; 3 mL/min; retention time: 10–11 min). The product fraction was formulated with phosphate-buffered saline (pH 7) and *p*-aminobenzoate as a radiostabilizer. The specific activity of the product was in the range of 1,800–1,900 GBq/μmol at the end of synthesis.

The radiochemical purity of the injectate, determined by high-performance liquid chromatography, was greater than 95%.

Preparation of Tumor-Bearing Mice

All animal studies were approved by and performed in compliance with the U.K. Home Office guidelines. U87-MG cells (catalog no. HTB-14; American Type Culture Collection) were grown in McCoy 5a medium (M8403; Sigma-Aldrich) supplemented with 10% fetal bovine serum. Cells were passaged twice per week, at 70%–80% confluence, and incubated in 5% CO_2 at 37°C. Male CD-1 nude mice (~20 g; Charles River U.K. Ltd.) were injected subcutaneously in the nape of the neck with a suspension of 10^6 U87-MG cells. Tumors were allowed to develop for approximately 3 wk (100–200 mm^3) before the dosing regimen was begun.

Dosing Regimen

At 3 wk after inoculation of U87-MG tumor cells, the mice were divided into 2 treatment groups. One group received sunitinib (0.2-mL volume containing ~1.2 mg of free base) at a dose of 60 mg/kg by oral gavage; the second group received oral administrations of the vehicle alone (water containing hydrochloric acid [at a molar ratio of 1:1.02], 0.5% polysorbate, 10% polyethylene glycol, and sodium hydroxide [to adjust the pH to between pH 3.3 and pH 3.7]). The tumor-bearing animals were treated with sunitinib or the vehicle alone on a 5-day-on, 2-day-off treatment cycle previously described by de Bouard et al. (*26*). Sunitinib was well tolerated; no significant effects on animal health were observed.

Small-Animal PET and micro-CT

Small-animal PET was performed with a microPET-P4 system (Siemens Inc.). Images were generated from sinogram data and rebinned to a 2-dimensional format by use of the Fourier rebinning algorithm and 2-dimensional filtered backprojection. The small-animal PET scanner was calibrated in terms of absolute activity concentration (kBq/cm^3) by imaging of a phantom approximating the dimensions of a mouse body and filled with a known concentration of ^{18}F-fluoride.

The U87-MG xenograft model animals were imaged by use of the small-animal PET camera with either a "dynamic" (0–90 min after injection) or a "static" (70–90 min after injection) imaging protocol to quantify tumor and reference tissue uptake of ^{18}F-fluciclatide. Animals imaged with the dynamic imaging protocol were anesthetized with isoflurane anesthetic (maintained at a 2% alveolar concentration) and placed on a flat imaging bed routinely used for PET studies. A transmission scan was obtained with a ^{57}Co source before injection of the animals via a lateral tail vein with approximately 10 MBq of ^{18}F-fluciclatide (0.1-mL injection containing ~0.1 μg of peptide) in an injection volume of not more

than 5 mL/kg. On injection the dynamic acquisition was commenced. The animals were maintained under anesthesia throughout the imaging sequence. Both the respiration and the temperature of the animals were monitored by use of a BioVET system (m2m Imaging Corporation, US).

Animals imaged with the static imaging protocol were injected via the lateral tail vein with approximately 10 MBq of ^{18}F-fluciclatide in an injection volume of not more than 5 mL/kg. The animals were placed in a holding cage; at the appropriate time point, the animals were anesthetized and placed on an imaging bed. After a transmission scan was obtained, a 20-min static scan (70–90 min after injection of ^{18}F-fluciclatide) under anesthesia was commenced. Once PET was complete, each animal was scanned with a micro-CT scanner to obtain anatomic information.

CT was performed with a MicroCAT II system (Siemens Inc.) at manufacturer-recommended settings (360° of rotation, 400-ms exposure time, the camera set at 40 kVp and 500 mA, and binning set at 4 × 4) to produce a resolution of 100 μm and a total radiation dose within safe exposure limits. Images were reconstructed with the image reconstruction, visualization, and analysis program supplied by the manufacturer.

Small-animal PET and CT data were analyzed with Amide software (SourceForge; http://amide.sourceforge.net). The PET and CT images were coregistered to confirm the anatomic locations of the tumors. The uptake of radioactivity in the tumors was determined by placement of a region of interest around the tumor border delineated on the CT images. A region of interest was also placed around a region of the muscle of the upper left forelimb as well as a region of the liver to provide reference tissue values. All imaging data are expressed as the percentage injected dose per gram (%ID/g). Images showing tumor uptake and whole-body uptake of radioactivity after ^{18}F-fluciclatide administration are [Fig. 1] presented in Figure 1.

The animals were imaged again with the same protocol on days 2, 7, 9, and 13 after initiation of the dosing regimen.

Microvessel Density (MVD) Measurement

On the final day of the study, after the acquisition of the scan, the animals were sacrificed, and the tumors were excised and fixed in neutral buffered formalin. The MVD of the tumors was quantified by use of a method described by Wedge et al. (*30*). Tumor specimens were fixed and stained for CD31 with a chromogen endpoint and analyzed in a masked manner (i.e., without knowledge of treatment assignment) with a KS400 instrument (Imaging Associates). MVD was calculated as the number of CD31-positive vessels per 5,000 μm^2 of viable tumor area in each tumor section.

RESULTS

Effect of Sunitinib on U87-MG Tumor Size

Throughout the study, the sizes of the tumors were measured by use of calipers, and the volumes of the tumors were calculated by use of the equation $a\times(b\times b)/2$, where a is the longest measurement and b is the shortest measurement. Figure 2 shows the average percentage change in [Fig. 2] maximum tumor volume from the baseline value (day 0, before sunitinib or vehicle administration) on each of the imaging days. From, and including, the day 7 data point, there was a trend toward a difference in tumor volumes between the sunitinib-treated group and the vehicle-treated group; however, because of the growth characteristics of this tumor type, the trend was not statistically significant at any time point ($P > 0.05$). Volumetric and diameter data were confirmed with CT measurements (data not shown).

Effect of Sunitinib on U87-MG Tumor Retention of ^{18}F-Fluciclatide

Small-animal PET and CT data were acquired on days 0, 2, 7, 9, and 13 after initiation of the dosing regimen (Fig. 3). [Fig. 3] The PET data showed that the level of tumor retention of ^{18}F-fluciclatide was significantly lower (2-way ANOVA with a post hoc Bonferroni test) in the sunitinib-treated group than in the vehicle-treated group from day 2 after therapy initiation onward. The level of tumor retention of ^{18}F-fluciclatide in the sunitinib-treated group decreased from that at day 0 (mean ± SEM: 1.5 ± 0.55 %ID/g) to 1.31 ± 0.56 %ID/g ($P < 0.05$) at day 2, 1.27 ± 0.48 %ID/g ($P < 0.05$) at day 7, 1.22 ± 0.53 %ID/g ($P < 0.01$) at day 9, and 1.12 ± 0.21 %ID/g ($P > 0.05$) at day 13. In comparison, the level of tumor retention of ^{18}F-fluciclatide in animals treated with vehicle alone increased from that at day 0 (1.28 ± 0.34 %ID/g) to 1.46 ± 0.44 %ID/g at day 2, 2.42 ± 0.73 %ID/g at day 7, 1.84 ± 0.64 %ID/g at day 9, and 1.88 ± 0.73 %ID/g at day 13. Overall, the change in tumor uptake of ^{18}F-fluciclatide from the baseline value in sunitinib-treated animals was significantly smaller (2-way ANOVA with a post hoc Bonferroni test) than that in vehicle-treated animals at 2 d (−23.6% vs. 20.7%; $P < 0.05$; 8 sunitinib-treated animals and 7 vehicle-treated animals), 7 d (−19.6% vs. 51.2%; $P < 0.05$; 4 sunitinib-treated animals and 2 vehicle-treated animals), and 9 d (−20.3% vs. 46.0%; $P < 0.01$; 7 sunitinib-treated animals and 8 vehicle-treated

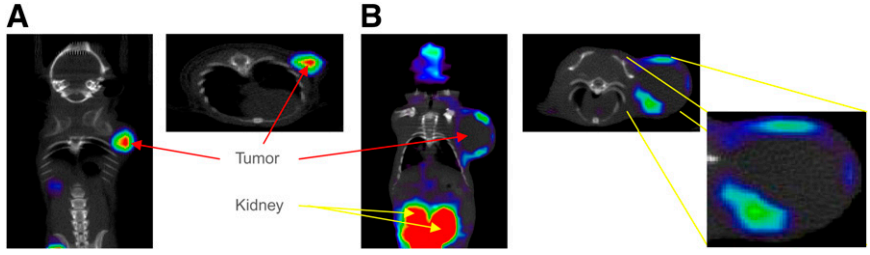

FIGURE 1. (A) Dynamic U87-MG tumor ^{18}F-fluciclatide distribution in sunitinib-treated animal displaying solid-core tumor. Retention of ^{18}F-fluciclatide was observed throughout whole tumor; highest level of accumulation was visible in core. (B) Dynamic U87-MG tumor ^{18}F-fluciclatide uptake in vehicle-treated animal displaying necrotic-core tumor (enlarged). Uptake and retention of ^{18}F-fluciclatide were limited primarily to peripheral regions of tumor; little uptake was observed in core.

RGB

RGB

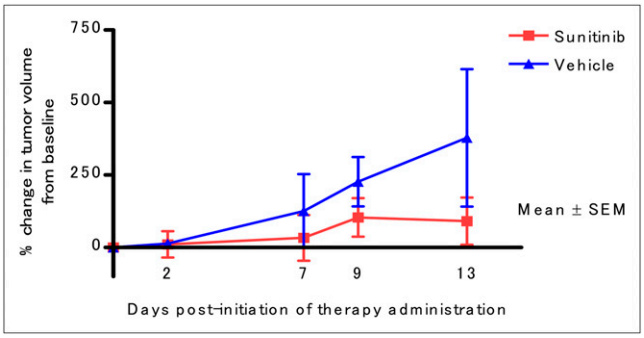

FIGURE 2. Percentage change in maximum tumor volume from baseline measurements (day 0). Level of growth of tumors in sunitinib-treated animals was lower than that in vehicle-treated animals from day 7 after initiation of sunitinib administration onward; however, this difference was not statistically significant ($P > 0.05$). Statistical analysis was done by use of 2-way ANOVA with post hoc Bonferroni test.

[**Fig. 4**] animals) after the initiation of sunitinib administration (Fig. 4). No significant differences in tumor uptake were observed at day 13 after inoculation because of the presence of necrosis in the vehicle-treated tumors, which decreased the %ID/g significantly (Fig. 1).

Skeletal muscle was used as a reference tissue for region-of-interest analysis, and the data demonstrated no significant differences in muscle uptake either before or after therapy. This result indicates that the decrease in tumor uptake observed with sunitinib therapy was specific.

Microvessel Density Analysis

[**Fig. 5**] Figure 5 shows representative tumor sections taken at 13 d after the initiation of sunitinib or vehicle administration and stained for endothelial cells with CD34 for the assessment of positively stained vessels per mm^2 of each section. The level of MVD, a measurement of angiogenesis, was significantly lower in tumors from sunitinib-treated mice than in those from control mice at 13 d after the initiation of therapy (39.2 ± 9.6 vs. 145.1 ± 17.5; $P = 0.0048$; 3 sunitinib-treated animals and 5 vehicle-treated animals; Student t test). This significant reduction in the level of MVD in the treated mice helped to confirm the therapeutic response of the tumors to sunitinib therapy and indicated that the concomitant reduction in ^{18}F-fluciclatide retention may have been at least partially due to the reduction in vascular density.

DISCUSSION

At present, tumor vasculature is quantified both preclinically and in surgical specimens by immunohistochemistry techniques. Because of the potential variability encountered in measuring MVD as well as the ethical and physical limitations of serial invasive procedures, such assays are often impractical in clinical trials (*31*). The inherent anatomic and physiologic heterogeneity of tumors means that multiple samples likely must be taken at any given time—another factor making such assays impractical in clinical trials. A noninvasive method for assessing tumor vascularity could obviate these technical challenges.

Previous studies demonstrated the utility of RGD-based radioligands for the noninvasive assessment of tumor vascularity and for assessment of the efficacy of single-dose antitumor therapy (*17,19,21,32,33*). However, relatively little attention has been focused on the ability of these radiotracers to monitor the response of tumors to therapies that target the vasculature longitudinally. Targeted antiangio-

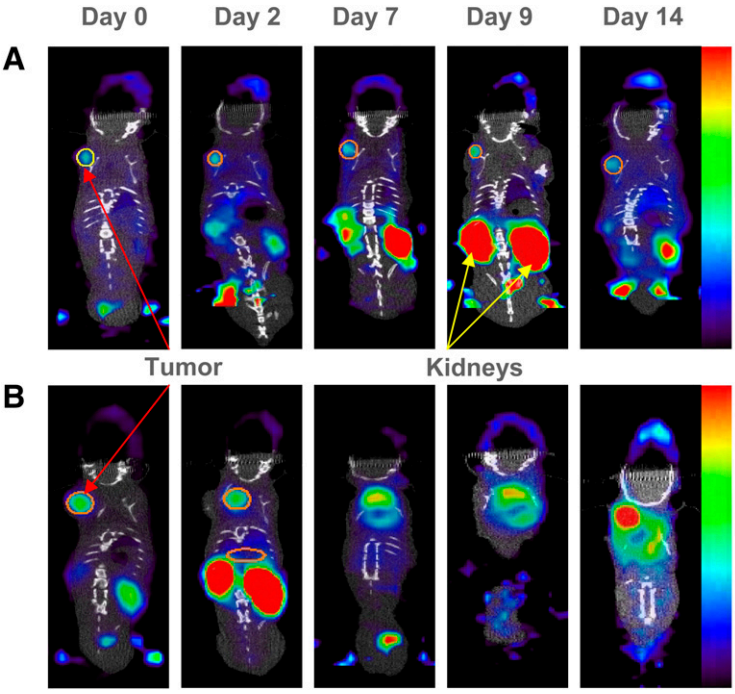

FIGURE 3. Representative coregistered small-animal PET and micro-CT images demonstrating uptake of ^{18}F-fluciclatide in U87-MG tumors in 1 sunitinib-treated animal (A) and 1 control animal (B) for duration of study. Retention of ^{18}F-fluciclatide in tumor (circled) of sunitinib-treated animal decreased significantly ($P < 0.05$) from day 2 onward. In comparison, ^{18}F-fluciclatide retention in control group tumors increased up to day 7 before decreasing slightly by day 13. Skeletal muscle, taken as reference tissue, showed no significant difference in ^{18}F-fluciclatide retention between groups on each day. Excretion of ^{18}F-fluciclatide was predominantly urinary (excretion via kidneys was evident on these images).

RGB

jnm077479-pe ■ 2/11/11

RGB

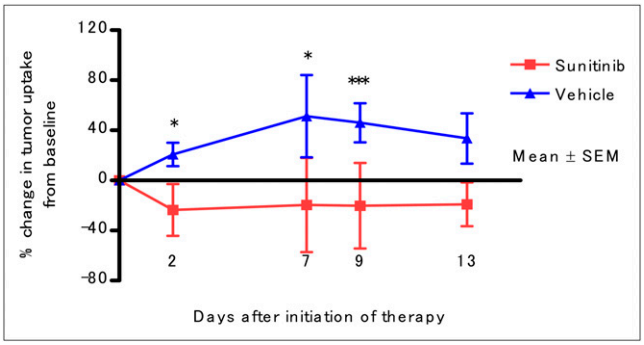

FIGURE 4. Graph showing percentage change in tumor uptake of ^{18}F-fluciclatide from baseline small-animal PET images (day 0). Level of tumor uptake of ^{18}F-fluciclatide in sunitinib-treated animals was significantly lower than that in vehicle-treated animals at 2 d (*$P < 0.05$), 7 d (*$P < 0.05$), and 9 d (***$P < 0.01$) after initiation of sunitinib administration. Statistical analysis was done by use of 2-way ANOVA with post hoc Bonferroni test.

genic therapies are becoming more widespread clinically and have been shown to have promise in the treatment of highly vascularized tumors, such as glioblastomas (*26*). In the present study, the ability of ^{18}F-fluciclatide to detect changes in tumor vascularity in tumor-bearing animals in response to antiangiogenic therapy was assessed over a 2-wk period.

The antiangiogenic agent sunitinib is an oral, small, molecular tyrosine kinase inhibitor that exhibits potent antiangiogenic and antitumor activities. Sunitinib is a rationally designed, highly bioavailable compound with nanomolar-range potency against antiangiogenic receptor tyrosine kinases, VEGFRs, and platelet-derived growth factor receptors (PDGFRs) (*34*). Because sunitinib inhibits both VEGFRs and PDGFRs, it simultaneously targets endothelial cells, pericytes, and glioblastoma cells expressing PDGFRs. Inhibition of receptor tyrosine kinases, VEGFRs, and PDGFRs has both direct and indirect regulatory effects on tumor growth, survival, and angiogenesis, consequently leading to a reduction in vascular development and hence in integrin expression or activation. In patients, sunitinib is typically administered as a single agent at a dose of 50 mg daily on a 4-week-on, 2-week-off treatment schedule.

The ability to quantitatively measure ^{18}F-fluciclatide binding to $\alpha_V\beta_3$-integrin and $\alpha_V\beta_5$-integrin expressed on both glioblastoma cells and the vasculature in response to sunitinib therapy allows for earlier confirmation of the response to therapy and is an early marker of tumor shrinkage. In the present study, a significant difference ($P < 0.05$) between the treated group and the control group was observed in terms of tumor retention of ^{18}F-fluciclatide from day 2 after inoculation onward; in contrast, when tumor size was assessed with calipers, a nonsignificant trend toward decreasing tumor volumes was observed. These data correlate well with our MVD data; that is, a significantly lower level of MVD expression was observed at day 13 in sunitinib-treated animals than in control animals. One limitation of the present MVD analysis was the lack of histopathologic data from tumors at early time points. A more complete understanding of tumor MVD at early stages after therapy initiation would further support the conclusion that early changes in ^{18}F-fluciclatide retention are due to the antiangiogenic effects of sunitinib.

The data from the present study showed that using ^{18}F-fluciclatide retention in tumors to measure $\alpha_V\beta_3$-integrin and $\alpha_V\beta_5$-integrin expression on glioblastoma cells and the vasculature allowed for a much earlier assessment of the response to therapy than the current standard method of measuring tumor shrinkage with calipers. Furthermore, assessment of tumor retention of ^{18}F-fluciclatide also revealed areas of necrosis in tumors, allowing further assessment of tumor integrity.

Our data are in agreement with those of recently published studies of the potential of targeting $\alpha_V\beta_3$-integrin and $\alpha_V\beta_5$-integrin expression as a marker of the response to therapy.

For example, in a study by Jung et al. (*32*), the uptake of a novel ^{99m}Tc-labeled glucosamino-RGD peptide was used to monitor the response to chemotherapy with paclitaxel (an antimicrotubule agent commonly used in the treatment of breast and non–small cell lung cancers (*35*)) in LLC tumor–bearing animals at approximately 4 wk after tumor inoculation. It was demonstrated that long-term paclitaxel therapy resulted in decreased LLC tumor uptake of the radiotracer, further supporting the use of the radiolabeled

RGB

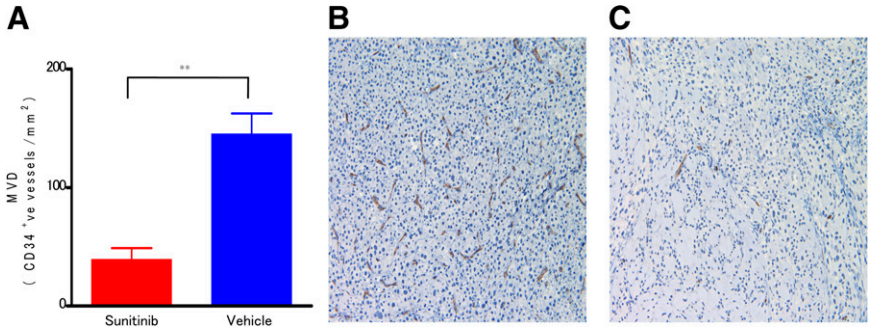

FIGURE 5. (A) Tumor MVD, measurement of angiogenesis, was significantly lower in tumors from sunitinib-treated mice than in control mice at 13 d after initiation of therapy administration (**$P < 0.05$). Representative tumor sections, taken at 13 d after initiation of sunitinib or vehicle administration (magnification, ×20), were analyzed for MVD after staining for endothelial cells with CD34. Higher level of staining (indicating vessels positive for CD34) was observed in tumor section from vehicle-treated (control) animal (B) than in tumor section from sunitinib-treated animal (C), indicative of increased vascular density. Statistical analysis was done by use of Student *t* test (mean ± SEM).

RGD peptide for monitoring the response to antiangiogenic therapy.

In a more recent study, Dumont et al. (*36*) used ^{64}Cu-DOTA-c(RGDfK) to monitor Src family kinase (SFK) expression in xenograft models in response to dasatinib therapy. Here, U87-MG xenograft–bearing animals were imaged at 72 h after dasatinib therapy. A reduction in tumor ^{64}Cu-DOTA-c(RGDfK) uptake of between ~40% and ~60% (in a dose-dependent response to therapy) was observed in treated animals, relative to that in control animals, with no observable differences in tumor sizes. However, the authors also found no differences in $\alpha_V\beta_3$-integrin expression between the treated group and the control group and concluded that dasatinib therapy acted to decrease integrin activation rather than expression, resulting in decreased ^{64}Cu-DOTA-c(RGDfK) binding.

The ability of ^{18}F-fluciclatide to target the neovasculature via the $\alpha_V\beta_3$-integrin and $\alpha_V\beta_5$-integrin receptors expressed on endothelial cells is supported by the work of Pasqualini et al. (*37*), who demonstrated that tumor vessels were the structural elements most targeted by the RGD sequence. However, a high level of expression of integrins on endothelial cells, relative to that on tumor cells, is not necessarily a feature for all tumors. Metastatic melanoma, for instance, has a high level of receptor expression. Beer et al. (*16*) demonstrated a higher level of expression of $\alpha_V\beta_3$-integrin on tumor cells than on the tumor vasculature in patients presenting with solid tumors, including melanomas, and imaged with ^{18}F-galacto-RGD. This high level of $\alpha_V\beta_3$-integrin expression on tumor cell lines was also confirmed preclinically with melanoma (M21) and glioblastoma (U87-MG) tumor cell lines (*38*). Further support is provided by the work of Zhang et al. (*39*), in which $\alpha_V\beta_3$-integrin receptors on the cell surface were measured and quantified (by sodium dodecyl sulfate–polyacrylamide gel electrophoresis and autoradiography) and shown to be highly expressed on both U87-MG tumor cells and activated endothelial cells (compared with other tumor cell types commonly used in xenograft models). The binding potential of ^{18}F-FRGD2, as determined by tracer kinetic analysis (after dynamic imaging), was measured and correlated with integrin expression on U87-MG tumors. It was noted that U87-MG tumors had the highest tumor tissue integrin and tumor cell integrin levels and, correspondingly, that U87-MG tumors had the highest initial uptake of radioactivity followed by rapid washout. It was also noted that this correlation between the binding potential and increased tracer uptake was especially improved at later time points (60 min after injection) compared with earlier time points, most likely because of increased perfusion and vascular permeability increasing nonspecific uptake.

Another limitation to the approach of targeting $\alpha_V\beta_3$-integrin and $\alpha_V\beta_5$-integrin is the potential for elevated uptake of RGD-based tracers in regions of inflammation. It was previously reported that, in patients with pigmented villonodular synovitis, the uptake of ^{18}F-galacto-RGD in inflammatory lesions can be intense and similar to the uptake observed in malignancies (*24*). This factor may be a shortcoming of the use of RGD-based tracers which, like ^{18}F-FDG, can show high uptake in inflammatory cells (*40*).

Overall, the data demonstrate the value of longitudinal PET; repeated imaging of the same subject allows the uptake of ^{18}F-fluciclatide to be measured longitudinally for rapid assessment of the response to therapy and the integrity of tumors. The assessment of tumor retention of the $\alpha_V\beta_3$-integrin– and $\alpha_V\beta_5$-integrin–targeting compound over time is significantly improved by this methodology, performed in individual animals, in comparison with current therapy standards (volumetric measurement and MVD analysis) (*31*).

CONCLUSION

Significant reductions in ^{18}F-fluciclatide tumor uptake were observed in sunitinib-treated animals, compared with vehicle-treated animals, before any significant changes in tumor size were detected. These studies suggest that ^{18}F-fluciclatide may have clinical utility in the detection of the tumor response to antiangiogenic therapy earlier than current methods, which rely on the measurement of changes in tumor size or biopsy.

ACKNOWLEDGMENTS

The authors would like to thank Pfizer, in particular, Donnie W. Owens, Sr. (Global Research & Development, Pfizer Inc.), for kindly supplying the sunitinib compound for use in these studies. We also thank Jon Shales and Maria Constantinou for the synthesis and supply of ^{18}F-fluciclatide as well as Rochelle Lear, Luisa Contreras Bravo, Clare Durrant, and Joanne Cooper for their help.

REFERENCES

1. Hynes RO. A re-evaluation of integrins as regulators of angiogenesis. *Nat Med.* 2002;8:918–921.
2. Brooks PC, Clark RA, Cheresh DA. Requirement of vascular integrin alpha v beta 3 for angiogenesis. *Science (New York, NY).* 1994;264:569–571.
3. Hood JD, Cheresh DA. Role of integrins in cell invasion and migration. *Nat Rev.* 2002;2:91–100.
4. Carmeliet P, Jain RK. Angiogenesis in cancer and other diseases. *Nature.* 2000;407:249–257.
5. Bishop GG, McPherson JA, Sanders JM, et al. Selective $\alpha_v\beta_3$-receptor blockade reduces macrophage infiltration and restenosis after balloon angioplasty in the atherosclerotic rabbit. *Circulation.* 2001;103:1906–1911.
6. Chavakis E, Riecke B, Lin J, et al. Kinetics of integrin expression in the mouse model of proliferative retinopathy and success of secondary intervention with cyclic RGD peptides. *Diabetologia.* 2002;45:262–267.
7. Creamer D, Sullivan D, Bicknell R, Barker J. Angiogenesis in psoriasis. *Angiogenesis.* 2002;5:231–236.
8. Brooks PC. Role of integrins in angiogenesis. *Eur J Cancer.* 1996;32A(suppl): 2423–2429.
9. Giancotti FG, Ruoslahti E. Integrin signaling. *Science (New York, NY).* 1999; 285:1028–1032.
10. Horton MA. The alpha v beta 3 integrin "vitronectin receptor." *Int J Biochem Cell Biol.* 1997;29:721–725.
11. Kumar CC. Integrin alpha v beta 3 as a therapeutic target for blocking tumor-induced angiogenesis. *Curr Drug Targets.* 2003;4:123–131.
12. Friedlander M, Brooks PC, Shaffer RW, Kincaid CM, Varner JA, Cheresh DA. Definition of two angiogenic pathways by distinct alpha v integrins. *Science (New York, NY).* 1995;270:1500–1502.

13. Beer AJ, Haubner R, Wolf I, et al. PET-based human dosimetry of ^{18}F-galacto-RGD, a new radiotracer for imaging $\alpha_v\beta_3$ expression. *J Nucl Med.* 2006;47:763–769.
14. Bello L, Carrabba G, Giussani C, et al. Low-dose chemotherapy combined with an antiangiogenic drug reduces human glioma growth in vivo. *Cancer Res.* 2001;61:7501–7506.
15. Meitar D, Crawford SE, Rademaker AW, Cohn SL. Tumor angiogenesis correlates with metastatic disease, N-myc amplification, and poor outcome in human neuroblastoma. *J Clin Oncol.* 1996;14:405–414.
16. Beer AJ, Haubner R, Sarbia M, et al. Positron emission tomography using [^{18}F] galacto-RGD identifies the level of integrin $\alpha_v\beta3$ expression in man. *Clin Cancer Res.* 2006;12:3942–3949.
17. Beer AJ, Niemeyer M, Carlsen J, et al. Patterns of $\alpha_v\beta_3$ expression in primary and metastatic human breast cancer as shown by ^{18}F-galacto-RGD PET. *J Nucl Med.* 2008;49:255–259.
18. Chen X, Tohme M, Park R, Hou Y, Bading JR, Conti PS. Micro-PET imaging of alphavbeta3-integrin expression with ^{18}F-labeled dimeric RGD peptide. *Mol Imaging.* 2004;3:96–104.
19. Haubner R. Alphavbeta3-integrin imaging: a new approach to characterise angiogenesis? *Eur J Nucl Med Mol Imaging.* 2006;33(suppl 1):54–63.
20. Haubner R, Decristoforo C. Radiolabelled RGD peptides and peptidomimetics for tumour targeting. *Front Biosci.* 2009;14:872–886.
21. Liu S, Hsieh WY, Jiang Y, et al. Evaluation of a ^{99m}Tc-labeled cyclic RGD tetramer for noninvasive imaging integrin $\alpha_v\beta3$-positive breast cancer. *Bioconjug Chem.* 2007;18:438–446.
22. Kenny LM, Coombes RC, Oulie I, et al. Phase I trial of the positron-emitting Arg-Gly-Asp (RGD) peptide radioligand ^{18}F-AH111585 in breast cancer patients. *J Nucl Med.* 2008;49:879–886.
23. Dobrucki LW, de Muinck ED, Lindner JR, Sinusas AJ. Approaches to multimodality imaging of angiogenesis. *J Nucl Med.* 2010;51(suppl 1):66S–79S.
24. Haubner R, Weber WA, Beer AJ, et al. Noninvasive visualization of the activated alphavbeta3 integrin in cancer patients by positron emission tomography and [^{18}F]galacto-RGD. *PLoS Med.* 2005;2:e70.
25. Chow LQ, Eckhardt SG. Sunitinib: from rational design to clinical efficacy. *J Clin Oncol.* 2007;25:884–896.
26. de Bouard S, Herlin P, Christensen JG, et al. Antiangiogenic and anti-invasive effects of sunitinib on experimental human glioblastoma. *Neuro Oncol.* 2007;9:412–423.
27. Faivre S, Demetri G, Sargent W, Raymond E. Molecular basis for sunitinib efficacy and future clinical development. *Nat Rev Drug Discov.* 2007;6:734–745.
28. Indrevoll B, Kindberg GM, Solbakken M, et al. NC-100717: a versatile RGD peptide scaffold for angiogenesis imaging. *Bioorg Med Chem Lett.* 2006;16:6190–6193.
29. Glaser M, Morrison M, Solbakken M, et al. Radiosynthesis and biodistribution of cyclic RGD peptides conjugated with novel [^{18}F]fluorinated aldehyde-containing prosthetic groups. *Bioconjug Chem.* 2008;19:951–957.
30. Wedge SR, Kendrew J, Hennequin LF, et al. AZD2171: a highly potent, orally bioavailable, vascular endothelial growth factor receptor-2 tyrosine kinase inhibitor for the treatment of cancer. *Cancer Res.* 2005;65:4389–4400.
31. Hlatky L, Hahnfeldt P, Folkman J. Clinical application of antiangiogenic therapy: microvessel density, what it does and doesn't tell us. *J Natl Cancer Inst.* 2002;94:883–893.
32. Jung KH, Lee KH, Paik JY, et al. Favorable biokinetic and tumor-targeting properties of ^{99m}Tc-labeled glucosamino RGD and effect of paclitaxel therapy. *J Nucl Med.* 2006;47:2000–2007.
33. Morrison MS, Ricketts SA, Barnett J, Cuthbertson A, Tessier J, Wedge SR. Use of a novel Arg-Gly-Asp radioligand, ^{18}F-AH111585, to determine changes in tumor vascularity after antitumor therapy. *J Nucl Med.* 2009;50:116–122.
34. Mendel DB, Laird AD, Xin X, et al. In vivo antitumor activity of SU11248, a novel tyrosine kinase inhibitor targeting vascular endothelial growth factor and platelet-derived growth factor receptors: determination of a pharmacokinetic/pharmacodynamic relationship. *Clin Cancer Res.* 2003;9:327–337.
35. Horwitz SB. Taxol (paclitaxel): mechanisms of action. *Ann Oncol.* 1994;5(suppl 6):S3–S6.
36. Dumont RA, Hildebrandt I, Su H, et al. Noninvasive imaging of alphaVbeta3 function as a predictor of the antimigratory and antiproliferative effects of dasatinib. *Cancer Res.* 2009;69:3173–3179.
37. Pasqualini R, Koivunen E, Ruoslahti E. Alpha v integrins as receptors for tumor targeting by circulating ligands. *Nat Biotechnol.* 1997;15:542–546.
38. Haubner R, Wester HJ, Weber WA, et al. Noninvasive imaging of $\alpha_v\beta3$ integrin expression using ^{18}F-labeled RGD-containing glycopeptide and positron emission tomography. *Cancer Res.* 2001;61:1781–1785.
39. Zhang X, Xiong Z, Wu Y, et al. Quantitative PET imaging of tumor integrin $\alpha_v\beta_3$ expression with ^{18}F-FRGD2. *J Nucl Med.* 2006;47:113–121.
40. Kubota R, Yamada S, Kubota K, Ishiwata K, Tamahashi N, Ido T. Intratumoral distribution of fluorine-18-fluorodeoxyglucose in vivo: high accumulation in macrophages and granulation tissues studied by microautoradiography. *J Nucl Med.* 1992;33:1972–1980.